2

ARMY RESEARCH LABORATORY

# A HIFX Electron-Beam Dosimetry System

by Gregory K. Ovrebo, Steven M. Blomquist, and
Steven R. Murrill

ARL-TR-363

February 1994

# REPORT DOCUMENTATION PAGE

*Form Approved OMB No. 0704-0188*



| 1. AGENCY USE ONLY *(Leave blank)* | 2. REPORT DATE | 3. REPORT TYPE AND DATES COVERED |
|---|---|---|
| | February 1994 | Final, from 1 Jan. to 31 Dec. 1993 |

**4. TITLE AND SUBTITLE**
A HIFX Electron-Beam Dosimetry System

**5. FUNDING NUMBERS**
PE: 62120

**6. AUTHOR(S)**
Gregory K. Ovrebo, Steven M. Blomquist, and Steven R. Murrill

**7. PERFORMING ORGANIZATION NAME(S) AND ADDRESS(ES)**
U.S. Army Research Laboratory
Attn: AMSRL-WT-NG
2800 Powder Mill Road
Adelphi, MD 20783-1197

**8. PERFORMING ORGANIZATION REPORT NUMBER**
ARL-TR-363

**9. SPONSORING/MONITORING AGENCY NAME(S) AND ADDRESS(ES)**
U.S. Army Research Laboratory
2800 Powder Mill Road
Adelphi, MD 20783-1197

**10. SPONSORING/MONITORING AGENCY REPORT NUMBER**

**11. SUPPLEMENTARY NOTES**
AMS code: 612120.H250011
ARL PR: 3FE728

**12a. DISTRIBUTION/AVAILABILITY STATEMENT**
Approved for public release; distribution unlimited.

**12b. DISTRIBUTION CODE**

**13. ABSTRACT** *(Maximum 200 words)*

The U.S. Army Research Laboratory has developed a dosimetry system for use with the High-Intensity Flash X-ray (HIFX) facility and the custom low-noise test fixture used to perform radiation tests of integrated circuits in vacuum. When the flash x-ray is used in its electron-beam mode, dose rates greater than $10^{13}$ rads(Si)/s are achievable. This dose rate is above the useful limit of more conventional dosimetric methods, such as thermoluminescent dosimeters (TLD's). Our method, which uses chromel-constantan thermocouples to measure electron beam intensity, also eliminates the necessity of breaking vacuum between shots to replace dosimeters, a process that greatly reduces the number of shots performable per day. This paper describes the dosimetry system and the results of experiments and calculations that correlate thermocouple voltages and radiation dose. We also describe methods of varying the dose rate of the HIFX electron beam.

**14. SUBJECT TERMS**
Electrons, dosimetry, theromocouples, flash x-ray

**15. NUMBER OF PAGES**
24

**16. PRICE CODE**

| 17. SECURITY CLASSIFICATION OF REPORT | 18. SECURITY CLASSIFICATION OF THIS PAGE | 17. SECURITY CLASSIFICATION OF ABSTRACT | 20. LIMITATION OF ABSTRACT |
|---|---|---|---|
| Unclassified | Unclassified | Unclassified | UL |

NSN 7540-01-280-5500

Standard Form 298 (Rev. 2-89)
Prescribed by ANSI Std. Z39-18
298-102

## Contents



### Appendices



### Figures



### Table

# 1. Introduction

The Army Research Laboratory (ARL) has developed a capability for survivability testing of integrated circuits (IC's) that uses the High Intensity Flash X-ray (HIFX) test facility in the electron-beam mode, together with the low-noise test fixture of the U.S. Army Space and Strategic Defense Command (USASSDC). This capability allows for testing of both application-specific integrated circuits (ASIC's) and standard IC's with electron dose rates of $10^{13}$ rads(Si)/s and higher.

At these high dose rates, thermoluminescent dosimeters (TLD's) are at the limit of their usefulness and are clumsy to use in an evacuated test chamber. To avoid these problems, we have designed and fabricated an electron-beam dosimetry system that employs thermocouples with junctions in the beam path to measure the surface dose due to the HIFX electron beam. We have tested this dosimetry system, measured its response when exposed to varying electron fluences, and compared those responses to measurements of dose provided by TLD's in standard containers. We provide some guidelines for varying the dose at the test device by changing the configuration of the test apparatus. Finally, we discuss how to use these thermocouple dose measurements to calculate the dose in the region of interest in the test device.

# 2. Methodology

## 2.1 Materials

The materials and tools used to perform this experiment were as follows:

- a Tektronix DSA 602 digitizing oscilloscope;
- two Tektronix 7A22 differential amplifiers modified to work with the DSA 602;
- a Tektronix 11A32 two-channel amplifier;
- two Omega chromel-constantan (type E) micro-thermocouple assemblies in 0.020-in. 304 stainless steel sheaths with ungrounded junctions;
- Harshaw manganese-doped calcium fluoride ($CaF_2$:Mn) thermoluminescent chip dosimeters;
- a Harshaw TLD reader;
- the Integrated TIGER Series one-dimensional radiation transport code, version 2.1;*

**Distributed by the Radiation Shielding Information Center, Oak Ridge National Laboratory.*

- 6-in.-diameter AK vacuum tubing;
- the USASSDC/JAYCOR low-noise ASIC test fixture;
- a vacuum-tight adapter joining the test fixture to AK tubing; and
- the HIFX test facility in electron-beam mode.

## 2.2 Procedures

This experiment consisted of two parts:

1. Tests at HIFX to determine the correlation between paired thermocouples in the electron-beam path during the shot with the readings of TLD's just behind the thermocouples.
2. Radiation transport calculations to model the thermocouple response to irradiation by the HIFX electron beam.

### *2.2.1 Thermoluminescent Dosimetry Measurements*

The Omega thermocouples were attached to the adapter that joined the AK vacuum tubing to the test fixture. We positioned the thermocouple junctions at the center of the electron beam from opposite sides of the adapter by feeding the sheathed thermocouples through small holes drilled at a slant into the adapter. The holes were sealed with RTV silicone rubber adhesive sealant. The thermocouple output leads were connected to the center posts of ungrounded plastic BNC bulkhead connectors. The BNC's were connected to twinaxial cables fed through a port between the test cell and the HIFX screen room. Each twinaxial cable supplied a signal to a differential amplifier in the DSA 602 digitizing oscilloscope, eliminating most common-mode noise. We recorded both signals on the oscilloscope during each shot.

The flash x-ray was operated in its electron-beam mode (without bremsstrahlung converter) at the standard charging voltage of 4.1 MV. The electron beam traveled down an evacuated drift tube attached to the HIFX machine and connected to the test fixture by a vacuum-tight adapter. An aluminum aperture near the entrance to the drift tube controls the beam diameter. A lead-aluminum-lead collimator on the adapter restricts the area exposed. Figure 1 shows the experimental configuration of HIFX and the test fixture. Figure 2 is a diagram of the arrangement of collimator, thermocouples, and the TLD canister.

Before each shot, three $CaF_2$ TLD's were placed in an aluminum capsule 0.5 in. in diameter with walls 0.030 in. thick. The TLD canister was then attached to the adapter and placed in the center of the beam path, just behind the thermocouple junctions. After the TLD canister was put in place,

Figure 1. Diagram of test setup, with drift tube connecting HIFX and ETS test fixture.

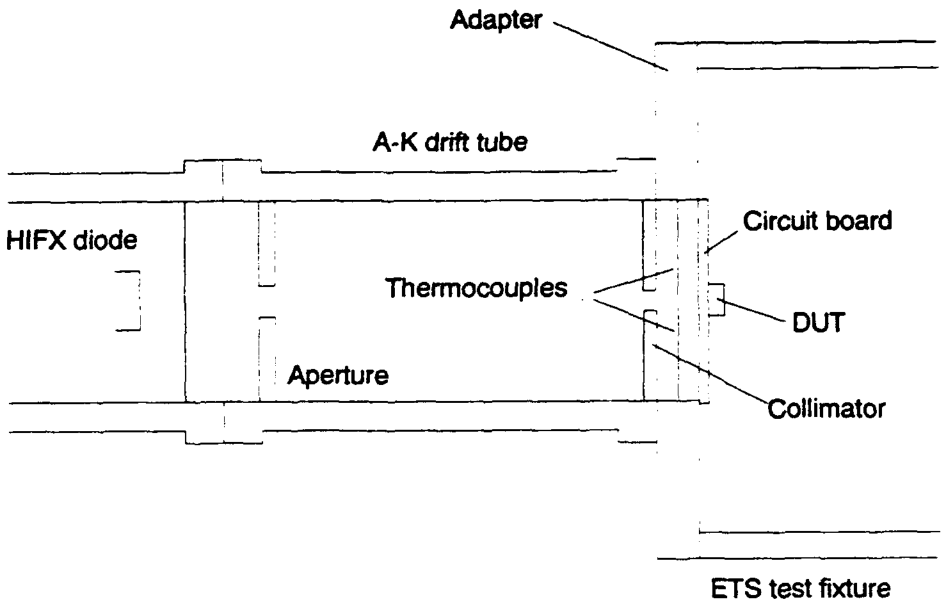


Figure 2. Cross-section view of collimator, thermocouples, and TLD canister.

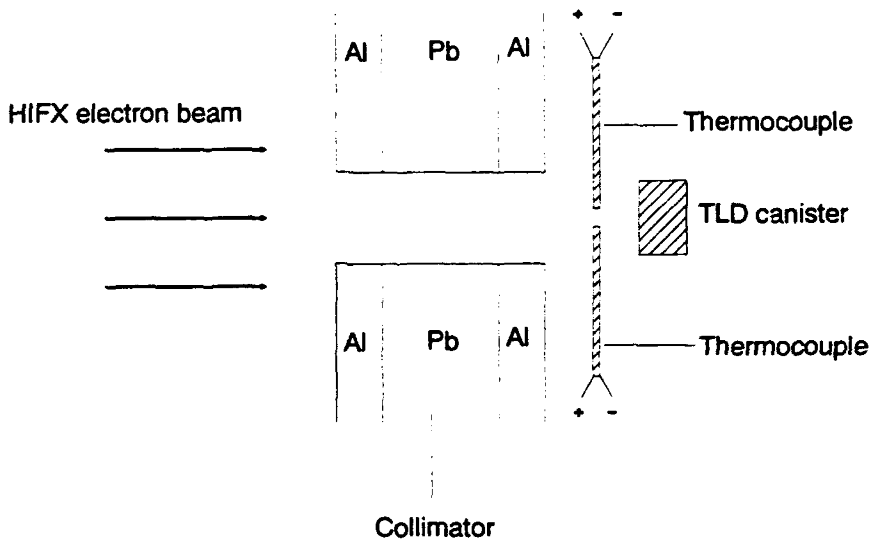


the vacuum drift tube was closed and pumped down to approximately $5 \times 10^{-6}$ torr before firing. This pump-down took about 15 minutes.

After the shot, the signal traces were examined and stored in the scope's memory, their maximum excursion was determined, and a hard copy of the signals was produced. The TLD's were retrieved and read.

Two variables were available for adjusting the dose seen at the thermocouple position: drift tube length and aperture diameter. One can vary drift tube length by connecting several sections of AK tubing; sections ranging in lengths from 5 to 120 cm are available. We chose drift tubes 15, 35, and 60 cm long. Apertures are made from 0.25-in.-thick aluminum plate; about 20 different diameters are available. We chose apertures of 0.250, 0.422, and 0.625 in.

### 2.2.2 *Thermocouple Response Simulations*

We used TIGER, the one-dimensional radiation transport code from the Integrated TIGER Series, to model the voltage response of the chromel-constantan thermocouples to electron-beam irradiation. TIGER was used to determine the relationship between dose in the thermocouple junction and dose in the $CaF_2$ TLD chip when it was exposed to the HIFX electron beam. The voltage response to dose deposition in the thermocouple wire was calculated from the specific heat of the metal and from tables of thermoelectric voltage for the type E thermocouples.

# 3. Results

TLD dose information reported here is given in terms of dose($CaF_2$), rather than in terms of the more customary dose(Si). Dose($CaF_2$) is the energy per unit mass deposited in the TLD, independent of source or spectrum. The HIFX TLD reader gives results in dose(Si) by multiplying dose($CaF_2$) by a correction factor (0.979), which is specific to the HIFX *photon* spectrum. Thus, the correction factor is not strictly applicable to the HIFX *electron* spectrum that we are using.

In order to convert the dose($CaF_2$) to dose in the region and material of interest for the HIFX electron spectrum, one must perform a radiation transport calculation (with a program like the TIGER Monte Carlo code[1]) to determine the energy deposition in the region of interest in the test object.

## 3.1 Experimental Results

Because the response of these TLD's is limited to dose levels below 200,000 rads($CaF_2$), only 15 of the total 24 HIFX shots could be used to correlate thermocouple response to TLD readings. The data from those 15 shots are shown in table 1. The complete tabulation from all 24 shots, including errors, is given in appendix A.

Thermocouple response is plotted against measured dose for all HIFX shots that yielded usable TLD data (i.e., all shots for which all TLD's read less than their limiting value of 200 krads($CaF_2$)). The responses of the two thermocouples are averaged to give one data point per shot. The plotted points fall on a best-fit line whose slope is 0.988 $\mu$V/krad($CaF_2$), with a standard deviation of 0.0103 $\mu$V/krad($CaF_2$). Figure 3 shows the plot of the data points and the best-fit line through them.

[1] *J. A. Halbleib and T. A. Hehlhorn, ITS: The Integrated TIGER Series of Coupled Electron/Photon Monte Carlo Transport Codes, Report No. SAND84-0573, Sandia National Laboratories, Albuquerque, New Mexico (1984).*

| Shot no. | Drift length (cm) | Aperture (in.) | TLD dose (krads($CaF_2$)) | Thermocouple response ($\mu$V) |
|---|---|---|---|---|
| 7399 | 15 | 0.250 | 77.9 | 72.0 |
| 7400 | 15 | 0.250 | 90.2 | 91.0 |
| 7401 | 15 | 0.250 | 76.4 | 76.0 |
| 7402 | 15 | 0.250 | 67.2 | 72.0 |
| 7405 | 15 | 0.422 | 170.9 | 169.0 |
| 7409 | 60 | 0.625 | 38.6 | 38.0 |
| 7410 | 60 | 0.625 | 36.3 | 37.0 |
| 7411 | 60 | 0.625 | 25.1 | 27.0 |
| 7412 | 60 | 0.250 | 4.4 | 4.0 |
| 7413 | 60 | 0.422 | 14.7 | 13.5 |
| 7414 | 60 | 0.422 | 13.9 | 14.0 |
| 7415 | 60 | 0.422 | 14.1 | 14.0 |
| 7416 | 35 | 0.422 | 36.1 | 34.0 |
| 7417 | 35 | 0.422 | 39.7 | 35.0 |
| 7418 | 35 | 0.422 | 37.6 | 35.0 |

**Table 1. Measured dose and thermocouple response in HIFX electron beam.**

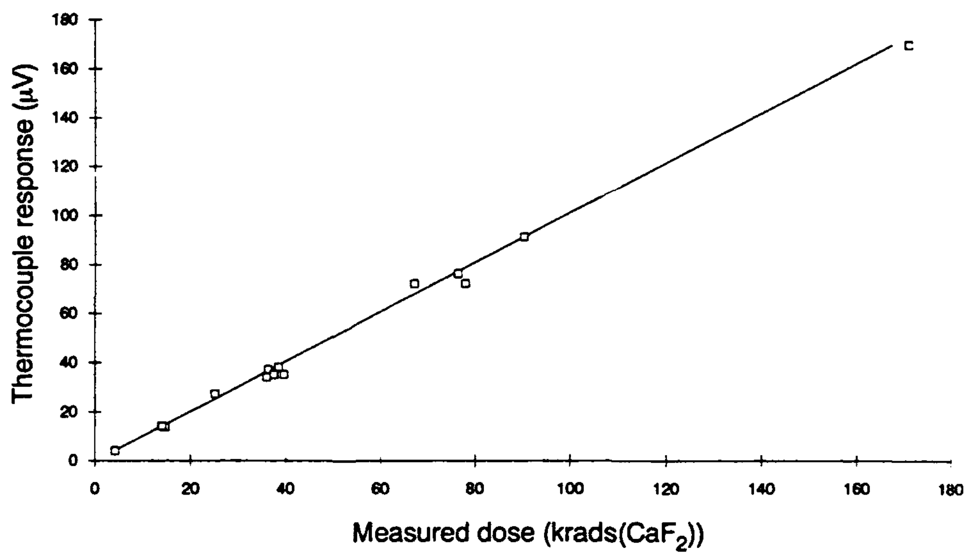


**Figure 3. Averaged thermocouple responses to HIFX electron beam are plotted against $CaF_2$ dose as measured by TLD's. Best-fit line has a slope of 0.988 $\mu$V/krad($CaF_2$).**

After the conclusion of HIFX testing, bench testing with the Tektronix DSA 602 digitizing oscilloscope and Tektronix 7A22 differential amplifier plug-ins revealed a systematic error in the data: the amplifiers are nonlinear at low input voltages. We took measurements to determine the magnitude of the error. A calibrated input signal from an oscilloscope was attenuated to 200 to 250 μV and fed to the 7A22 plug-ins in the DSA 602; the scope signal was measured and compared with the calibrated input signal. This measurement was repeated with three different calibrated signals from two different types of oscilloscopes. The measured signal was an average of 22 percent higher than the calibrated input signal, with a standard deviation of 6 percent. This correction yields a true thermocouple response of 0.81 μV/ krad($CaF_2$). Any measurements made with other data acquisition apparatus must take this correction into account.

We can draw some conclusions about the relationship between the electron-beam dose and beam variables like the aperture area and the drift tube length. We can also use the correlation factor we derived, 0.988 μV/ krad($CaF_2$), to calculate the dose in cases where it is too high for conventional TLD measurements.

One might hypothesize that, within limits, the dose is proportional to the area of the aperture. Figure 4 shows the dose plotted against the aperture area for a 15-cm drift tube. Figure 5 shows the dose plotted against the aperture area for a 60-cm drift tube. In both cases, the data show that the dose does vary approximately as the area of the aperture.

We can also make some observations about the relationship between the HIFX electron beam dose and drift tube length. Figure 6 shows dose plotted against the inverse square of the drift tube length in the case of the 0.422-in. diameter aperture. It appears that the dose varies approximately as the inverse square of drift tube length.

**Figure 4. Dose in rads($CaF_2$) as a function of aperture area for 15-cm drift tube.**

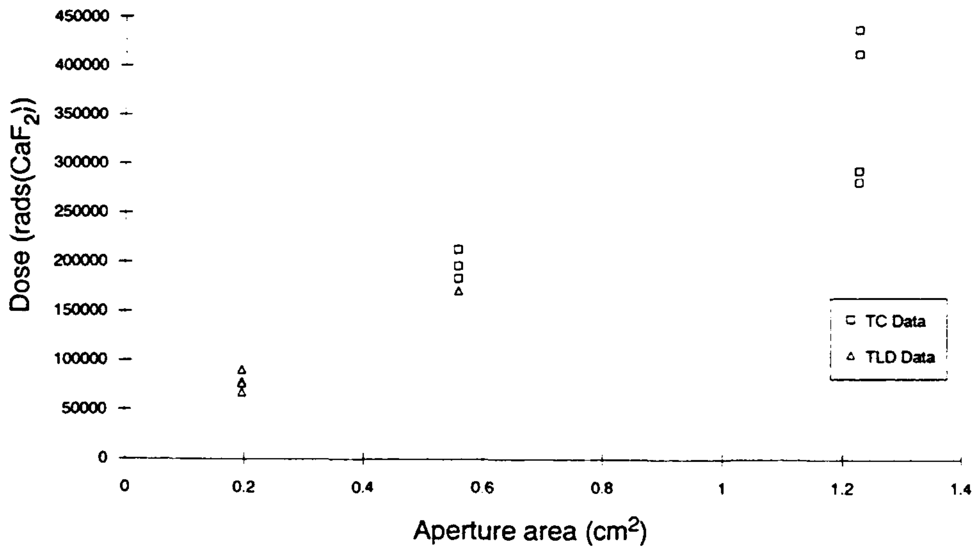

**Figure 5. Dose in rads($CaF_2$) as a function of aperture area for 60-cm drift tube.**

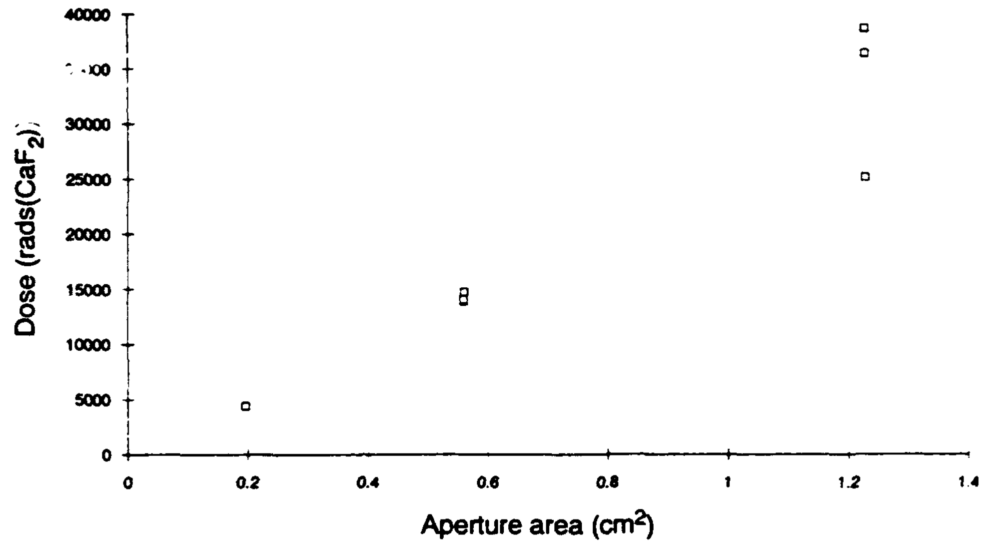


**Figure 6. Dose in rads($CaF_2$) as a function of inverse square of drift tube length for a 0.422-in.-diameter aperture.**

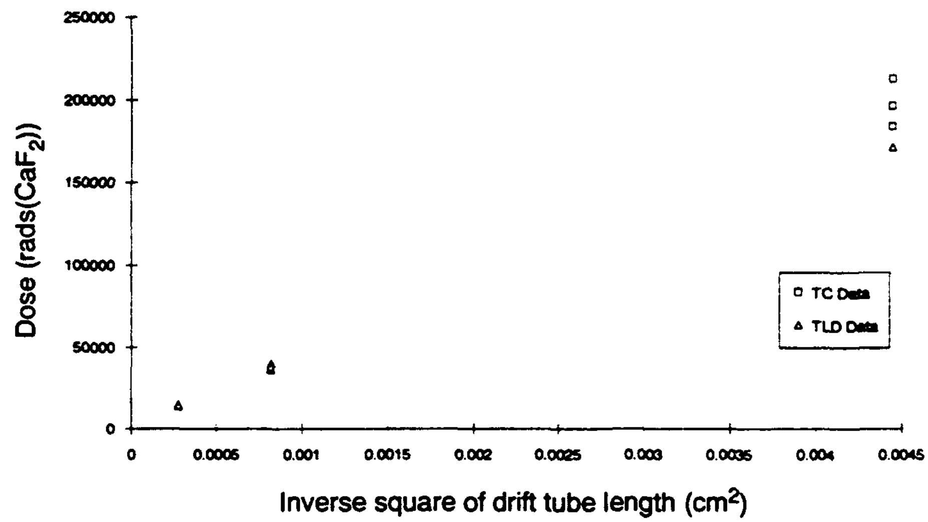


## 3.2 Computer Modeling Results

In order to model the voltage response of the thermocouples as a function of dose($CaF_2$), we first calculate the voltage response due to dose deposited in the thermocouple material. The thermoelectric voltage of the chromel-constantan thermocouples near room temperature is 61 μV/°C. The combined specific heat of the chromel-constantan wires is 0.103 cal/g-°C at room temperature (chromel is 80 percent nickel and 20 percent chrome; constantan is 55 percent nickel and 45 percent copper); the specific heat of the stainless steel 304 sheath is 0.11 cal/g-°C; the specific heat of the magnesium oxide insulator inside the sheath is 0.21 cal/g-°C. The mass-weighted specific heat of the entire thermocouple assembly is 0.133 cal/g-°C. The ratio of thermoelectric voltage to specific heat, converted to

rads(thermocouple), is 1.1 μV/krad. We used TIGER to calculate energy deposition in both the thermocouple assembly and in a $CaF_2$ chip TLD in the aluminum canister. We calculate the energy deposition in the thermocouple assembly by averaging the energy deposition in all layers of the slab, weighted by the mass thickness in g/cm$^2$. More information about this calculation is provided in appendix B. These numbers allow us to convert from rads(thermocouple) to rads($CaF_2$). We can then calculate the radiation response:

$$R(\mathrm{CaF_2}) = 1.1\ \mu\mathrm{V/krad(thermocouple)} \times \frac{D(\mathrm{thermocouple})}{D(\mathrm{CaF_2})}\ .$$

The TIGER simulation calculates the ratio of $D$(thermocouple) to $D(CaF_2)$ to be 0.92. Thus the TLD-thermocouple correlation factor derived from the simulation is 1.01 μV/krad($CaF_2$).

## 3.3 Experimental and Calculation Error

Calculation of the correlation between thermocouple response and TLD dose measurement yielded the value 0.988 μV/krad($CaF_2$). The sources of error in this calculation are the error in TLD measurement (±0.0577 percent for the mean of three TLD's, each of which has an individual error of ±10 percent), and the error in measurement of the thermocouple voltages (which has a maximum of ±15 percent). The combined error is calculated to be

$$S = \sqrt{(0.15)^2 + (0.0577)^2} = 0.16\ ,$$

for an estimated error of ±16 percent. Taking into account the systematic error caused by the differential amplifiers yields a thermocouple response of 0.81 μV/krad($CaF_2$); the combined error is

$$S = \sqrt{(0.15)^2 + (0.0577)^2 + (0.06)^2} = 0.17\ ,$$

for an estimated error of ±17 percent.

Computer modeling of thermocouple radiation response yielded the value 1.01 μV/krad($CaF_2$). Sources of error in this calculation are the estimated error in thermocouple voltage response (±2 percent), the estimated error in the thermocouple specific heat (±5 percent), the estimated error in the calculated thermocouple dose based on calculations of differing geometries (±15 percent), and estimated error in the calculated TLD dose (±5 percent). The total error in the calculated thermocouple response is

$$S = \sqrt{(0.02)^2 + (0.05)^2 + (0.15)^2 + (0.05)^2} = 0.17\ ,$$

for an estimated error of ±17 percent.

The measured thermocouple response has an upper error bound of 0.81 μV/krad($CaF_2$) + 17 percent, or 0.95 μV/krad($CaF_2$). The calculated thermocouple response has a lower error bound of 1.01 μV/krad($CaF_2$) – 17 percent, or 0.84 μV/krad($CaF_2$). The error bounds overlap, giving a reasonable agreement between measurement and prediction.

# 4. Discussion and Conclusion

The careful experimenter must not confuse the external dose measured by the dosimetry system with the dose inside the device at the *region of interest*, usually a silicon layer in an IC chip. These dose numbers will differ because of radiation attenuation/enhancement by the surrounding materials (such as device packaging) and the different energy absorption characteristics of the dosimeter and the material of interest.[2] Therefore, a calculation must be performed with a code like the Integrated TIGER Series if we wish to relate the measured external dose to the dose in the region of interest.

The calculation of dose in the region of interest has two parts. First, dose in a $CaF_2$ TLD in an aluminum canister outside the device package is compared with the dose in an identical TLD inside the device package at the position of the chip. This calculation provides the dose($CaF_2$) at the point of interest. Second, to obtain dose(Si) at the chip, we compare the dose in a TLD inside the package to the dose in a silicon layer inside the package. This process can be expressed in the following equation:

$$D(\mathrm{Si})_{\mathrm{device}} = D(\mathrm{CaF_2})_{\mathrm{measured}} \times \frac{D(\mathrm{CaF_2})_{\mathrm{package}}}{D(\mathrm{CaF_2})_{\mathrm{can}}} \times \frac{D(\mathrm{Si})_{\mathrm{package}}}{D(\mathrm{CaF_2})_{\mathrm{package}}} ,$$

or

$$D(\mathrm{Si})_{\mathrm{device}} = D(\mathrm{CaF_2})_{\mathrm{measured}} \times \frac{D(\mathrm{Si})_{\mathrm{package}}}{D(\mathrm{CaF_2})_{\mathrm{can}}} .$$

Therefore, once we have used the thermocouples to measure $D(\mathrm{CaF_2})_{\mathrm{measured}}$, we need only calculate the dose in an external TLD and the dose in the silicon layer in order to derive the dose(Si) at the location of the chip. Figure 7 is a graph of the HIFX electron energy spectrum. Figure 8 shows a diagram of the materials included in each step of the calculation.

[2]*Steven R. Murrill, C. Wesley Tipton, and Charles T. Self, An Electron-Beam Dose Deposition Experiment: TIGER 1-D Simulation Code versus Thermoluminescent Dosimetry, Harry Diamond Laboratories, HDL-TM-91-3 (1991), pp 1–2.*

Figure 7. HIFX electron energy spectrum.

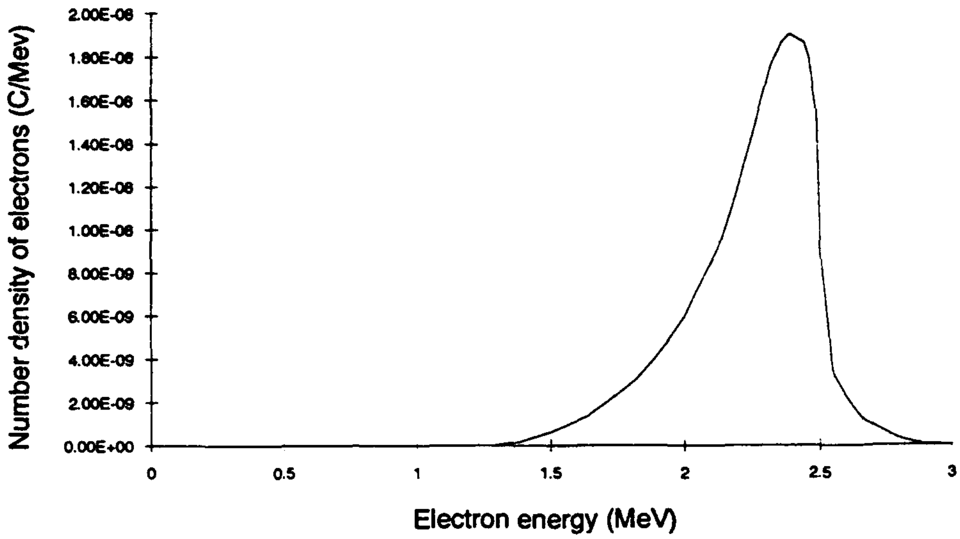


Figure 8. Slab geometries used in TIGER calculations of dose in silicon layer of interest in device:
(a) TLD in canister and
(b) silicon in package.

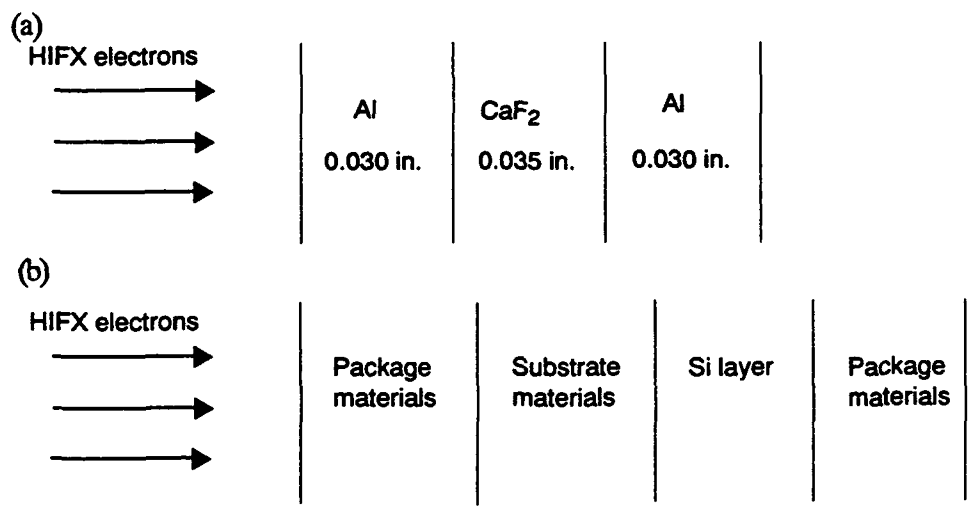


# Acknowledgments

We wish to thank James Blackburn for many useful discussions related to this work, and the staff of the High Intensity Flash X-ray facility for their assistance in the performance of the testing.

# Appendix A. Dosimetry Data

Table A-1 is a complete listing of data from the correlation of the High Intensity Flash X-ray (HIFX) electron-beam thermocouple response to thermoluminescent dosimeter (TLD) readings. The variables from shot to shot are the drift tube length and the aperture diameter. TLD results are shown, where they are valid, including the mean of the three TLD readings from each shot and the error on that mean value (5.77 percent). The mean TLD dose($CaF_2$) is multiplied by a correction factor of 0.979 to yield dose(Si). The response of each thermocouple, in millivolts, is listed, as well as the mean thermocouple response for each shot and the measurement error for that mean response.

It should be noted that no TLD readings are reported for a shot when any of the TLD's showed levels above 200 krads($CaF_2$). The TLD's are not calibrated above this level. In such cases, the average dose is replaced with the extrapolated dose (in boldface), which is calculated from the thermocouple response and the correlation factor derived from this experiment.

Note also that readings from shots 7397 and 7398 are much lower than those from the previous two shots, although drift tube length and aperture size were unchanged. We believe that the aperture had fallen out of alignment between the second and third shots, so that it was off center and tilted. It was found in this position after the fourth shot; this would explain the anomalously low readings on the third shot as well.

**Table A-1. Shot data for test of thermocouple dosimetry system.**

| Shot no. | Tube length (cm) | Aperture (in.) | TLD dose (rads(Si)) | | | | Ave TLD dose (rads($CaF_2$)) | TLD error (rads($CaF_2$)) | Thermocouple voltage (mV) | | | |
|---|---|---|---|---|---|---|---|---|---|---|---|---|
| | | | TLD 1 | TLD 2 | TLD 3 | Ave | | | TC1 | TC2 | Ave TC | TC error |
| 7395 | 15 | 0.625 | — | — | — | **403,695.3** | **412,354.8** | — | 0.400 | 0.400 | 0.400 | 0.0141 |
| 7396 | 15 | 0.625 | — | — | — | **427,917.0** | **437,096.1** | — | 0.404 | 0.444 | 0.424 | 0.0028 |
| 7397 | 15 | 0.625 | — | — | — | **286,623.7** | **292,771.9** | — | 0.268 | 0.300 | 0.284 | 0.0028 |
| 7398 | 15 | 0.625 | — | — | — | **275,522.1** | **281,432.1** | — | 0.256 | 0.290 | 0.273 | 0.0014 |
| 7399 | 15 | 0.250 | 72,587.2 | 81,425.1 | 74,822.2 | 76,278.2 | 77,914.4 | 4498.4 | 0.064 | 0.072 | 0.068 | 0.0028 |
| 7400 | 15 | 0.250 | 94,263.4 | 80,861.4 | 89,705.9 | 88,276.9 | 90,170.5 | 5206.0 | 0.086 | 0.096 | 0.091 | 0.0014 |
| 7401 | 15 | 0.250 | 72,669.5 | 76,217.3 | 75,434.4 | 74,773.7 | 76,377.7 | 4409.7 | 0.074 | 0.078 | 0.076 | 0.0014 |
| 7402 | 15 | 0.250 | 61,646.5 | 68,797.4 | 66,852.2 | 65,765.4 | 67,176.1 | 3878.4 | 0.070 | 0.074 | 0.072 | 0.0014 |
| 7403 | 15 | 0.422 | — | — | — | **207,903.1** | **212,362.7** | — | 0.204 | 0.208 | 0.206 | 0.0014 |
| 7404 | 15 | 0.422 | — | — | — | **179,644.4** | **183,497.9** | — | 0.174 | 0.182 | 0.178 | 0.0014 |
| 7405 | 15 | 0.422 | 149,373.9 | 185,333.6 | 167,253.7 | 167,320.4 | 170,909.5 | 9867.5 | 0.164 | 0.174 | 0.169 | 0.0014 |
| 7406 | 15 | 0.422 | — | — | — | **191,755.3** | **195,868.5** | — | 0.188 | 0.192 | 0.190 | 0.0014 |
| 7407 | 15 | 0.625 | — | — | — | **360,298.1** | **368,026.6** | — | 0.352 | 0.362 | 0.357 | 0.0014 |
| 7408 | 15 | 0.625 | — | — | — | **367,362.7** | **375,242.8** | — | 0.358 | 0.370 | 0.364 | 0.0014 |
| 7409 | 60 | 0.625 | 36,121.6 | 39,320.6 | 37,844.2 | 37,762.1 | 38,572.1 | 2227.0 | 0.038 | 0.038 | 0.038 | 0.0014 |
| 7410 | 60 | 0.625 | 31,967.8 | 33,569.2 | 41,079.3 | 35,538.8 | 36,301.1 | 2095.8 | 0.036 | 0.038 | 0.037 | 0.0014 |
| 7411 | 60 | 0.625 | 27,223.6 | 22,303.8 | 24,138.6 | 24,555.3 | 25,082.1 | 1448.1 | 0.026 | 0.028 | 0.027 | 0.0014 |
| 7412 | 60 | 0.250 | 4,177.1 | 3,951.7 | 4,669.3 | 4,266.0 | 4,357.5 | 251.6 | 0.004 | 0.004 | 0.004 | 0.0007 |
| 7413 | 60 | 0.422 | 15,114.6 | 13,640.3 | 14,455.9 | 14,403.6 | 14,712.6 | 849.4 | 0.013 | 0.014 | 0.014 | 0.0007 |
| 7414 | 60 | 0.422 | 13,139.5 | 13,351.2 | 14,416.6 | 13,635.8 | 13,928.3 | 804.1 | 0.014 | 0.014 | 0.014 | 0.0007 |
| 7415 | 60 | 0.422 | 13,573.6 | 13,779.5 | 13,938.1 | 13,763.7 | 14,059.0 | 811.7 | 0.014 | 0.014 | 0.014 | 0.0007 |
| 7416 | 35 | 0.422 | 34,359.2 | 38,000.1 | 33,535.9 | 35,298.4 | 36,055.6 | 2081.7 | 0.032 | 0.036 | 0.034 | 0.0014 |
| 7417 | 35 | 0.422 | 43,517.3 | 34,020.2 | 38,994.9 | 38,844.1 | 39,677.4 | 2290.8 | 0.034 | 0.036 | 0.035 | 0.0014 |
| 7418 | 35 | 0.422 | 36,104.6 | 39,869.2 | 34,469.1 | 36,814.3 | 37,604.0 | 2171.1 | 0.034 | 0.036 | 0.035 | 0.0014 |

Bold = extrapolated dose

# Appendix B. One-Dimensional Radiation Transport Calculations

## B.1 TIGER Input

The following is a listing of the batch command file used to run a TIGER calculation of energy deposition in the chromel-constantan thermocouple assembly and in a $CaF_2$:Mn chip thermoluminescent dosimeter (TLD). The first section sets up a calculation of cross sections for the thermocouple and TLD materials for energies below 3 MeV. The next section is a one-dimensional calculation of electron and photon transport through the thermocouple and TLD, using the High Intensity Flash X-ray (HIFX) electron spectrum. This calculation includes energy deposition in each layer of the thermocouple-TLD slab. The final section is a calculation of the radiation transport through the TLD chip alone, including energy deposition in the $CaF_2$.

## Appendix B

```
$!
$! ++++++++++++++++++++++++++++++++++++++++++++++++++++
$! +                          +
$! +        TC_E.COM              +
$! + COMMAND FILE FOR RUNNING ITS ON HDL VAX-8800  +
$! +                          +
$! ++++++++++++++++++++++++++++++++++++++++++++++++++++
$!
$ SET VERIFY
$ SET DEFAULT [SXTF.ITS]
$!
$! ++++++++++++++++++++PROGRAM XGEN++++++++++++++++++
$!
$!
$ ASSIGN/USER XDATA.LIB FOR009:
$! [CROSS SECTION DATA IS ON FOR009:]
$ ASSIGN/USER TC_EXSEC.DAT FOR011:
$! [INPUT FOR ITS IS ON FOR011:]
$ ASSIGN/USER TRANSX.OUT FOR006:
$! [PRINTED OUTPUT IS ON FOR006:]
$!
$ RUN X
*------------------*
TITLE
— CROSS-SECTION, ELECTRONS THROUGH THERMOCOUPLE, TLD W/AL PACKAGE —
ENERGY 3.0
MATERIAL FE 0.72 CR 0.19 NI 0.09 DENSITY 7.75        * STAINLESS STEEL
MATERIAL O 0.40 MG 0.60 DENSITY 3.57                 * MgO
MATERIAL NI 0.675 CU 0.225 CR 0.10 DENSITY 8.7 * THERMOCOUPLE, TYPE E
MATERIAL N GAS
MATERIAL AL
MATERIAL F 0.484 CA 0.495 MN 0.021 DENSITY 3.18* TLD
MATERIAL SI
*------------------*
$!
$ DELETE FOR007.DAT;*
$ PURGE X.EXE
```

```
$!
$! +++++++++++++++++++PROGRAM ITS++++++++++++++++++
$!
$!
$ DELETE MTIG.TMP;*
$! [DELETES THE MTIG.TMP;9 LEFT OVER FROM THE LAST JOB.]
$!
$ ASSIGN/USER TC_EXSEC.DAT FOR011:
$! [CROSS SECTION DATA FROM XDATA IS ON FOR011:]
$ ASSIGN/USER TC_E.OUT FOR006:
$! [PRINTED OUTPUT IS ON FOR006:]
$ ASSIGN/USER MTIG.DMP FOR010:
$! [MTIG.DMP WILL CONTAIN DUMP FILE FOR RESTART, IF NECESSARY.]
$ ASSIGN/USER MTIG.TMP FOR012:
$! [MTIG.TMP WILL CONTAIN INTERMEDIATE BATCH OUTPUTS.]
$!
$ RUN M
*______________________*
TITLE
—HIFX electrons transported through 4 mil thermocouple, TLD—
********* GEOMETRY *********
GEOMETRY 8
* MAT NZONE THIK ECUT PTCZ
1 1 0.00762
2 1 0.00762
3 1 0.02032
2 1 0.00762
1 1 0.00762
5 1 0.0762
6 1 0.0889
5 1 0.0762
********* SOURCE *********
ELECTRONS
SPECTRUM 33
1.000 .9996 .9985 .9967 .9866 .9764 .9587 .9552 .9504 .9262 .9029
.8497 .8150 .6980 .6364 .5539 .4914 .4195 .3390 .3077 .2625 .1914
.1577 .1149 .0917 .0664 .0441 .0310 .0208 .0062 .00355 .00084 .00
```

## Appendix B

```
2.999 2.889 2.822 2.775 2.666 2.611 2.552 2.543 2.534 2.504 2.487
2.459 2.442 2.388 2.359 2.319 2.286 2.244 2.189 2.164 2.124 2.047
2.002 1.931 1.884 1.821 1.748 1.693 1.636 1.504 1.461 1.382 1.29
CUTOFFS 0.015 0.005
********* OUTPUT OPTIONS *********
********* OTHER OPTIONS *********
HISTORIES 10000
*————————————————————————*
NEW-DATA-SET
TITLE
—HIFX electrons transported through TLD—
********* GEOMETRY *********
GEOMETRY 3
* MAT NZONE THIK ECUT PTCZ
5 1 0.0762
6 1 0.0889
5 1 0.0762
********* SOURCE *********
ELECTRONS
SPECTRUM 33
1.000 .9996 .9985 .9967 .9866 .9764 .9587 .9552 .9504 .9262 .9029
.8497 .8150 .6980 .6364 .5539 .4914 .4195 .3390 .3077 .2625 .1914
.1577 .1149 .0917 .0664 .0441 .0310 .0208 .0062 .00355 .00084 .00
2.999 2.889 2.822 2.775 2.666 2.611 2.552 2.543 2.534 2.504 2.487
2.459 2.442 2.388 2.359 2.319 2.286 2.244 2.189 2.164 2.124 2.047
2.002 1.931 1.884 1.821 1.748 1.693 1.636 1.504 1.461 1.382 1.29
CUTOFFS 0.015 0.005
********* OUTPUT OPTIONS *********
********* OTHER OPTIONS *********
HISTORIES 10000
$!
$!
$ DELETE FOR011.DAT;*
$ PURGE MTIG.TMP
$ PURGE M.EXE
$!
```

-

## B.2 TIGER Output

The following is a listing of the pertinent parts of the TIGER output, the energy deposition due to the HIFX electron beam (including secondary electrons and bremsstrahlung photons). The first section is for the thermocouple in front of a TLD in an aluminum capsule. The first column gives the number of the material layer, or zone, starting with the layer nearest the HIFX machine. The second column gives the type of material in each zone, as defined in the TIGER input file. Note that zone 1 is the outer sheath of the thermocouple, zone 2 is the MgO insulator, zone 3 is the chromel-constantan thermocouple, zone 4 is MgO, and so on. The next column gives the zone boundaries in terms of *Z/R*, the zone thickness divided by the maximum electron range in that material. Zone boundaries are described in the next column in terms of the range, the product of zone thickness and material density, with units g/cm$^2$. The next four columns give calculated energy deposition in each layer due to primary electrons, knock-on electrons, and photon-produced secondary electrons, and the total energy deposition in each layer, in units of MeV-cm$^2$/g-source particle. The "Total" below each energy deposition column is the sum of the products of energy deposition (MeV-cm$^2$/g-source particle) and range (g/cm$^2$) for each zone. At the bottom of the page is the calculated energy deposition for a TLD in a 30-mil-thick aluminum package.

One obtains the weighted average of the energy deposition in the thermocouple assembly by multiplying the energy deposition in each zone by the zone thickness (in g/cm$^2$), summing the products, and dividing by the total thickness. Table B-1 provides a summary.

**Table B-1. Energy deposition summary.**

| Zone | Zone thickness (g/cm$^2$) | Energy deposition (MeV-cm$^2$/g-electron) | Energy deposition (MeV/electron) |
|---|---|---|---|
| 1 | 0.0591 | 1.7948 | 0.1060 |
| 2 | 0.0272 | 2.4574 | 0.0668 |
| 3 | 0.1768 | 2.8410 | 0.5022 |
| 4 | 0.0272 | 3.4769 | 0.0946 |
| 5 | 0.0591 | 2.8013 | 0.1654 |
| Total | 0.3493 | — | 0.9351 |

$$\text{Average energy deposition} = \frac{0.9351\ \text{MeV/electron}}{0.3493\ \text{g/cm}^2}$$

$$= 2.68\ \text{MeV-cm}^2\text{/g-electron}\ .$$

Energy Deposition
(Normalized to one incident particle)

| | | Depth region | | (MeV-cm$^2$/g-source particle) | | | | | | | |
|---|---|---|---|---|---|---|---|---|---|---|---|
| Zone | Mat. | (*Z*/*R*) | (g/cm$^2$) | Prim | | Knock | | P-sec | | Total | |
| 1 | 1 | 0.0000E+00 – 2.9336E–02 | 0.0000E+00 – 5.9055E–02 | 1.8561E+00 | 1 | –6.7794E–02 | 15 | 6.5391E–03 | 10 | 1.7948E+00 | 1 |
| 2 | 2 | 2.9336E–02 – 4.4467E–02 | 5.9055E–02 – 8.6258E–02 | 2.4970E+00 | 1 | –4.2727E–02 | 28 | 3.1963E–03 | 26 | 2.4574E+00 | 1 |
| 3 | 3 | 4.4467E–02 – 1.3286E–01 | 8.6258E–02 – 2.6304E–01 | 2.8309E+00 | 0 | –8.0374E–03 | 36 | 1.8105E–02 | 6 | 2.8410E+00 | 0 |
| 4 | 2 | 1.3286E–01 – 1.4800E–01 | 2.6304E–01 – 2.9025E–01 | 3.4352E+00 | 2 | 4.0058E–02 | 63 | 4.3327E–03 | 31 | 3.4796E+00 | 2 |
| 5 | 1 | 1.4800E–01 – 1.7733E–01 | 2.9025E–01 – 3.4930E–01 | 2.7850E+00 | 1 | –2.1557E–03 | 99 | 1.8455E–02 | 6 | 2.8013E+00 | 1 |
| 6 | 5 | 1.7733E–01 – 2.8724E–01 | 3.4930E–01 – 5.5504E–01 | 2.5395E+00 | 1 | 7.9718E–03 | 27 | 5.9458E–03 | 12 | 2.5534E+00 | 1 |
| 7 | 6 | 2.8724E–01 – 4.4060E–01 | 5.5504E–01 – 8.3774E–01 | 1.5613E+00 | 1 | 3.9170E–03 | 27 | 7.2992E–03 | 10 | 1.5725E+00 | 1 |
| 8 | 5 | 4.4060E–01 – 5.5051E–01 | 8.3774E–01 – 1.0435E+00 | 5.6503E–01 | 2 | 1.2590E–03 | 36 | 3.6666E–03 | 12 | 5.6996E–01 | 2 |
| | | | Total (MeV) | 2.0160E+00 | 0 | –2.6179E–03 | 11 | 8.9226E–03 | 4 | 2.0223E+00 | 0 |

The energy conservation fraction is 0.1000225854925E+01 0

Energy Deposition
(Normalized to one incident particle)

| | | Depth region | | (MeV-cm$^2$/g-source particle) | | | | | | | |
|---|---|---|---|---|---|---|---|---|---|---|---|
| Zone | Mat. | (*Z*/*R*) | (g/cm$^2$) | Prim | | Knock | | P-sec | | Total | |
| 1 | 5 | 0.0000E+00 – 1.0991E–01 | 0.0000E+00 – 2.0574E–01 | 2.1021E+00 | 1 | –3.0442E–02 | 11 | 2.3111E–03 | 7 | 2.0740E+00 | 1 |
| 2 | 6 | 1.0991E–01 – 2.6327E–01 | 2.0574E–01 – 4.8844E–01 | 2.8892E+00 | 0 | 6.1848E–03 | 43 | 6.5362E–03 | 4 | 2.9020E+00 | 0 |
| 3 | 5 | 2.6327E–01 – 3.7318E–01 | 4.8844E–01 – 6.9418E–01 | 2.1175E+00 | 1 | 6.8209E–03 | 27 | 4.9405E–03 | 12 | 2.1293E+00 | 1 |
| | | | Total (MeV) | 1.6850E+00 | 0 | –3.1114E–03 | 12 | 3.3397E–03 | 4 | 1.6852E+00 | 0 |

The energy conservation fraction is 0.1000053490268E+01 0

## Distribution

Administrator
Defense Tech Information Ctr
Attn: DTIC-DDA (2 copies)
Cameron Station, Building 5
Alexandria, VA 22304-6145

Director
Defense Nuclear Agency
Attn: RAEE, L. Cohn
6801 Telegraph Road
Alexandria, VA 22310-3398

U.S. Army Corps of Engineers
Attn: CEHND-SY, J. Loyd
PO Box 1600
Huntsville, AL 35807-4301

U.S. Army Space & Strategic Defense Command
Attn: CSSD-SD-AM, D. Stott
PO Box 1500
Huntsville, AL 35807-3801

Commanding Officer
Naval Weapons Support Center
Attn: Code 6054, T. Turflinger
Bldg. 2506
Crane, IN 47522

Sandia National Laboratories, 2154
Attn: T. Wrobel
PO Box 5800
Albuquerque, NM 87185

IBM Corp, Federal Systems Division
Attn: B. Posey
9500 Godwin Drive
Manassas, VA 22110

Physitron
Attn: M. Christopher
3304 Westmill Drive
Huntsville, AL 35805

Physitron
Attn: J. Azarewicz
16885 Via del Campo Court, Suite 200
San Diego, CA 92127

U.S. Army Research Lab
Attn: AMSRL-OP-SD-TL, Tech Library (3 copies)
Attn: AMSRL-OP-SD-TM, Mail & Records Mgmt
Attn: AMSRL-OP-SD-TP, Tech Pub
Attn: AMSRL-WT-NG, Chief
Attn: AMSRL-WT-NG, W. Lilley
Attn: AMSRL-WT-NG, D. Robertson
Attn: AMSRL-WT-NG, G. Ovrebo (10 copies)
Attn: AMSRL-WT-NG, H. Eisen
Attn: AMSRL-WT-NG, J. Blackburn
Attn: AMSRL-WT-NG, J. Vanderwall
Attn: AMSRL-WT-NG, S. Blomquist
Attn: AMSRL-WT-NG, S. Murrill (10 copies)
Attn: AMSRL-WT-NG, C. W. Tipton
Attn: AMSRL-WT-NH, G. Huttlin
Attn: AMSRL-WT-NH, K. Kerris
Attn: AMSRL-WT-NH, M. Litz